THE JOURNAL OF BIOLOGICAL CHEMISTRY VOL. 286, NO. 18, pp. 16374–16385, May 6, 2011
Printed in the U.S.A.

Heme Oxygenase-1 Couples Activation of Mitochondrial Biogenesis to Anti-inflammatory Cytokine Expression*[S]

Received for publication, November 29, 2010, and in revised form, March 16, 2011 Published, JBC Papers in Press, March 18, 2011, DOI 10.1074/jbc.M110.207738

Claude A. Piantadosi[‡§¶‖1], Crystal M. Withers[¶], Raquel R. Bartz[§], Nancy Chou MacGarvey[‡], Ping Fu[§], Timothy E. Sweeney[¶], Karen E. Welty-Wolf[‡‖], and Hagir B. Suliman[§]**

*From the Departments of [‡]Medicine, [§]Anesthesiology, and [¶]Pathology, Duke University Medical Center, Durham, North Carolina 27710 and the Departments of [‖]Medicine and **Anesthesiology, Durham Veterans Affairs Medical Center, Durham, North Carolina 27710*

The induction of heme oxygenase-1 (HO-1; *Hmox1*) by inflammation, for instance in sepsis, is associated both with an anti-inflammatory response and with mitochondrial biogenesis. Here, we tested the idea that HO-1, acting through the Nfe2l2 (Nrf2) transcription factor, links anti-inflammatory cytokine expression to activation of mitochondrial biogenesis. HO-1 induction after LPS stimulated anti-inflammatory IL-10 and IL-1 receptor antagonist (IL-1Ra) expression in mouse liver, human HepG2 cells, and mouse J774.1 macrophages but blunted tumor necrosis factor-α expression. This was accompanied by nuclear Nfe2l2 accumulation and led us to identify abundant Nfe2l2 and other mitochondrial biogenesis transcription factor binding sites in the promoter regions of *IL10* and *IL1Ra* compared with pro-inflammatory genes regulated by NF-κB. Mechanistically, HO-1, through its CO product, enabled these transcription factors to bind the core *IL10* and *IL1Ra* promoters, which for *IL10* included Nfe2l2, nuclear respiratory factor (NRF)-2 (Gabpa), and MEF2, and for *IL1Ra*, included NRF-1 and MEF2. In cells, *Hmox1* or *Nfe2l2* RNA silencing prevented IL-10 and IL-1Ra up-regulation, and HO-1 induction failed post-LPS in *Nfe2l2*-silenced cells and post-sepsis in Nfe2l2$^{-/-}$ mice. Nfe2l2$^{-/-}$ mice compared with WT mice, showed more liver damage, higher mortality, and ineffective CO rescue in sepsis. Nfe2l2$^{-/-}$ mice in sepsis also generated higher hepatic TNF-α mRNA levels, lower NRF-1 and PGC-1α mRNA levels, and no enhancement of anti-inflammatory *Il10*, *Socs3*, or *bcl-x$_L$* gene expression. These findings disclose a highly structured transcriptional network that couples mitochondrial biogenesis to counter-inflammation with major implications for immune suppression in sepsis.

Early survivors of severe sepsis often develop immune suppression (1, 2) and may later die with the multiple organ dysfunction syndrome (3). A key effector of multiple organ dysfunction syndrome is the liver, which is integral to the host response, especially in infections that activate Toll-like receptor 4 and NF-κB-dependent cytokine synthesis (4). The persistence of inflammatory cytokines such as TNF-α and IL-1β perpetuates immune activation, causing tissue damage and remodeling (5) and leads to sustained production of anti-inflammatory modulators and suppressors of adaptive immunity (6, 7).

These anti-inflammatory modulators include the type II cytokine IL-10, the soluble IL-1 receptor antagonist (sIL-1Ra)[2] (5), and SOCS (suppressor of cytokine signaling) proteins (8). IL-10 is widely expressed in the liver (9, 10) by Kupffer cells (11), stellate cells (12), and hepatocytes (13), where it contributes to LPS tolerance (14). The IL-10 receptor activates JAK/STAT (Janus kinase/signal transducer and activator of transcription) to block the production of TNF-α and other NF-κB-dependent mediators (15), the basis for its anti-inflammatory effects (16). IL-10 also suppresses mononuclear cell function (17), and IL-10 secretion by macrophages and neutrophils negatively regulates the response to LPS (18). Absence of IL-10 increases cytokine production (19, 20) and inflammation-induced mortality (21), which is reversed by restoration of IL-10 levels (22, 23).

Inflammation also induces HO-1, which metabolizes heme and releases CO, iron, and biliverdin (24), and promotes cell protection (25–27). HO-1 is involved in sepsis in macrophage IL-10 induction and suppression of TNF-α and nitric oxide synthase-2 (16, 28) but also mediates the anti-inflammatory effects of adiponectin in Kupffer cells (29) and activates mitochondrial biogenesis (30).

Mitochondrial damage without ischemia or hypoxia is experimentally and clinically well recognized in sepsis (31–34). During the resolution phase, energy homeostasis is restored by mitochondrial biogenesis (35–39) activated by innate immunity (37) as well as by electrophiles or oxidants that activate the basic leucine zipper transcription factor, Nfe2l2 (Nrf2) (40). Electrophiles free Nfe2l2 from its Keap1 docking protein, allowing it to enter the nucleus and induce xenobiotic and antioxidant genes (40), including *Hmox1* (41). Endogenous CO also stimulates mitochondrial H_2O_2 production (42), which acts as a retrograde signal for mitochondrial biogenesis in part through Nfe2l2 nuclear accumulation (30).

These findings suggest the hypothesis that HO-1/CO, acting through Nfe2l2, links anti-inflammatory gene expression to the transcriptional program for mitochondrial biogenesis. To test this hypothesis, we evaluated HO-1 and Nfe2l2 regulation and

* This work was supported, in whole or in part, by National Institutes of Health Grants AI064789 and GM084116.

[S] The on-line version of this article (available at http://www.jbc.org) contains supplemental Table S1 and Figs. S1–S3.

[1] To whom correspondence should be addressed: 0570 White Zone, CR II Building, Duke University Medical Center, Durham, NC 27710. Fax: 919-684-6002; E-mail: piant001@mc.duke.edu.

[2] The abbreviations used are: sIL-1Ra, soluble IL-1 receptor antagonist; HO-1, heme oxygenase-1; IL-1Ra, IL-1 receptor antagonist; NRF, nuclear respiratory factor; DCM/CO, CO-producing molecule dichloromethane; CREB, cAMP-response element-binding protein.

causal activation of mitochondrial biogenesis and anti-inflammation in cells challenged with LPS and in mice challenged with *Escherichia coli* sepsis. We also specifically investigated IL-10 and sIL-1Ra gene regulation by Nfe2l2 and other transcription factors of mitochondrial biogenesis, and in mice in sepsis, we also measured hepatic anti-inflammatory *Socs3* and *bcl-x_L* genes to check for their association with the mitochondrial biogenesis program. Evidence of an expanded network would signify the coupling of mitochondrial biogenesis to immune counter-regulation and implicate the genetic response to mitochondrial damage/repair as a factor in the apparent immune paralysis encountered in sepsis.

EXPERIMENTAL PROCEDURES

Materials—Primary antibodies were from Santa Cruz Biotechnology unless otherwise specified; secondary antibodies, including antibodies for fluorescence microscopy, were from Invitrogen. siRNA oligonucleotides were from Ambion. Mouse recombinant TNF-α, IL-10, *E. coli* LPS, and dichloromethane (DCM) were from Sigma.

Cells—Human HepG2 (hepatocellular carcinoma) cells were purchased from ATCC (Manassas, VA) and cultured in 5% CO_2 in RMPI 1640 (Hyclone) containing 10% FCS, 2 mM glutamine, 100 units/ml penicillin, and 100 μg/ml streptomycin. Studies were conducted in murine J774.1 macrophages (ATCC) at 85% confluence in RPMI 1640 supplemented with FCS. Both cell lines were exposed to LPS at 15 ng/ml and exposed to CO using the CO-producing molecule dichloromethane (DCM/CO; 50–100 μM), which generates CO through the cytochrome P450 system. Cells were transfected with scrambled (negative control) or targeted siRNA using FuGENE HD (Roche Applied Science) to achieve efficiencies of >70%.

Mice—The studies were approved by the Duke Institutional Animal Care and Use Committee. WT male C57BL/6 (The Jackson Laboratory) and Nfe2l2$^{-/-}$ mice (RIKEN) on a C57BL/6 background were used at 12–16 weeks of age. They were inoculated with 10^7 or 10^8 CFU live *E. coli* (serotype 086a: K61, ATCC, Rockville, MD) by peritoneal fibrin clot implantation followed by 1.5 ml of sterile 0.9% NaCl. This model activates hepatic mitochondrial biogenesis (37, 43). For CO exposures, mice breathed 250 or 500 ppm CO in air for 1 h (carboxyhemoglobin levels 10–20%) to induce mitochondrial biogenesis (42). At the appropriate times, mice were killed by isofluorane, and the livers were harvested and frozen at −80 °C.

Histology—Fresh livers were flushed with 0.9% cold NaCl, perfusion-fixed with 10% formalin, and divided into lobes. After 24 h, the livers were transferred to 70% ethanol and stored at 4 °C. The lobes were block-cut and embedded in paraffin, and 4-μm sections were randomly cut and stained with H&E and photographed at 200×.

Bioinformatics—Mouse and human *IL10* promoter loci were aligned, and DNA sequence homology was computed with the web-based Regulatory Visualization Tools for Alignment (rVISTA; www.gsd.lbl.gov/vista) (44, 45). Promoter analysis was performed with consensus transcription factor binding sequences located with DNASIS (Hitachi Software; Alameda, CA) and confirmed with MatInspector (Genomatix Software; München, Germany). Predicted binding sites for Nfe2l2/Nrf2 (accession no. NM_006164 (human); accession no. NM_010902 (mouse)), MEF2A (myocyte enhancer factor 2A, accession no. NM_001130926 (human); accession no. NM_001033713 (mouse)), NRF-1 (accession no. NM_005011 (human) and accession no. NM_001164226 (mouse)), and NRF-2α/Gabpa (accession no. NM_001197297 (human); accession no. NM_008065 (mouse)) of at least 85% homology were identified in human and mouse promoters.

ChIP and DNA Binding Assays—Nuclear liver and cell extracts were prepared as described (36, 37). Transcriptional activation of Nfe2l2 and MEF2A was measured using the TRANS-AM kit (Active Motif, Carlsbad, CA). ChIP assays were performed with ChIP-IT and Re-ChIP-IT kits (Active Motif) following the manufacturer's protocol (42). For liver, ~200 mg was diced on ice in PBS and fixed in 1% (v/v) formaldehyde at room temperature to cross-link protein to DNA. Reactions were stopped in 0.125 M glycine, the samples were centrifuged twice, and the final pellet was suspended in ChIP buffer. Genomic DNA was sheared by sonication, and lysates were tumbled overnight at 4 °C with salmon sperm DNA/protein A-agarose and anti-RNA polymerase II (Re-ChIP-IT), anti-MEF2, anti-Nfe2l2, and anti-NRF-1 (Cell Signaling) or normal rabbit IgG. Complexes were precipitated, washed, and eluted with 1% SDS and 100 mM $NaHCO_3$. After reversal of protein/DNA cross-linking, DNA was purified and amplified across the *IL10* and *IL1Ra* promoter regions of interest. ChIP samples were normalized to input chromatin (ΔCt) and enrichment defined as change in Ct in treated *versus* untreated samples (ΔCt), relative to IgG controls.

Protein Immunoblots—Liver homogenate, cell lysate, and nuclear extract proteins were separated by SDS-PAGE, and Western blots were performed. After the transfer, primary and secondary antibodies were applied, and the signals were developed using ECL. Blots were quantified in the mid-dynamic range, and the protein density was expressed relative to stable reference proteins.

Immunochemical Staining and Fluorescence Microscopy—For immunochemistry, cells were grown in one-well chamber slides to ~70% confluence. After reagent additions, the cells were washed in PBS, fixed in 2% paraformaldehyde, and washed with 1% Triton X-100 for 15 min at room temperature. Cells were labeled with primary antibodies to HO-1 (1:1000) and MEF2 (catalog no. sc-55500; 1:800). Fluorescence microscopy was performed on a Nikon H550S microscope (46).

Real-Time PCR—We performed qRT-PCR on an ABI PRISM 7000 system with TaqMan gene expression and premix assays (Applied Biosystems). 18 S rRNA served as an endogenous control. Quantification of gene expression was determined using the comparative threshold cycle CT and RQ method. The mt DNA copy number was determined by quantitative PCR using SYBR Green and the ABI system (42, 47).

Statistics—Grouped data are expressed as means ± S.E. for replicates of four to six. Significance was tested by an unpaired *t* test or with two-way analysis of variance using commercial software unless indicated otherwise. Statistical significance required $p < 0.05$.

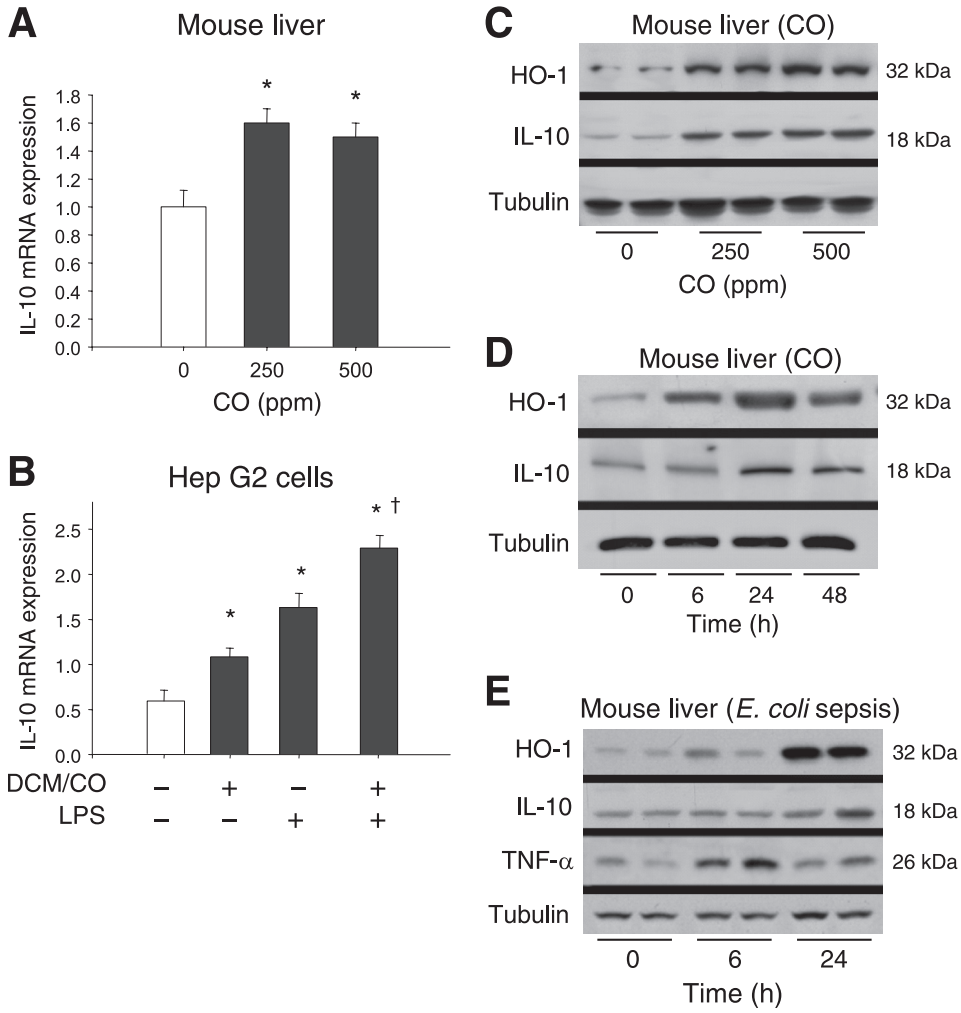

FIGURE 1. **Increases in IL-10 and HO-1 mRNA and protein expression after LPS and CO exposures.** *A*, increases in IL-10 mRNA levels in C57BL/6 mouse liver at 24 h after a 1-h exposure to CO at 250 or 500 ppm. *B*, increases in IL-10 mRNA levels in HepG2 cells 24 h after a 1-h exposure to DCM/CO (50 μM) or 24 h after LPS (10 ng); the combination of CO + LPS have an additive effect. *Error bars* indicate means ± S.E. of duplicate samples in triplicate experiments (*, $p < 0.05$ *versus* control; †, $p < 0.05$ *versus* control and LPS). *C*, Western blots of C57BL/6 mouse liver protein indicate dose increases in HO-1 and IL-10 levels at 24 h after 1-h exposures to 250 or 500 ppm CO. *D*, time course of hepatic HO-1 and IL-10 protein induction after 250 ppm CO. *E*, hepatic HO-1 and IL-10 induction after *E. coli* peritonitis in C57BL/6 mice. HO-1 is strongly up-regulated by 24 h; IL-10 is constitutive and increases at 24 h. TNF-α is shown for comparison.

RESULTS

HO-1/CO and LPS Activation of IL-10—HO-1 induction does not invariably stimulate *IL10*, so we confirmed that its CO product increases IL-10 mRNA levels in mouse liver, HepG2 cells, and J774.1 macrophages. In C57/BL/6 mice, 1 h of CO breathing (250 or 500 ppm) increased hepatic IL-10 mRNA levels by ~60% at 24 h (Fig. 1*A*). In HepG2 cells, DCM/CO at low μM levels doubled IL-10 mRNA content by 24 h (Fig. 1*B*). Comparably, LPS stimulated IL-10 production, and LPS + DCM/CO produced an additive effect. In J774.1 cells, IL-10 mRNA levels followed the same patterns, including after LPS + DCM/CO (data not shown).

Dose- and time-dependent increases in hepatic IL-10 and HO-1 protein levels after CO administration were documented by Western blot (Fig. 1, *C* and *D*). In an *E. coli* peritonitis model in mice, hepatic HO-1 protein levels were also significantly up-regulated at 24 h (Fig. 1*E*). IL-10 was constitutive and strongly up-regulated in sepsis but well after TNF-α production.

In HepG2 cells, DCM/CO or LPS challenge up-regulated HO-1 and IL-10 protein expression by 1–6 h. Peak responses for both occurred 24 h after these exposures (Fig. 2*A*). LPS + DCM/CO significantly enhanced HO-1 and IL-10 induction compared with either alone, whereas IL-10 up-regulation was blocked by *Hmox1* RNA silencing (Fig. 2*A*). HO-1 was thus required for increased IL-10 expression by DCM/CO and LPS. IL-10 (10 ng/ml) also induced cellular HO-1 expression within 6 h (Fig. 2*A*).

To show that LPS and CO up-regulate the transcriptional program of mitochondrial biogenesis in HepG2 cells, we measured protein for NRF-1 and the mitochondrial transcription factor A (Fig. 2*B*). Both proteins responded to both stimuli in a pattern similar to that of IL-10. IL-10 administration in HepG2 cells inhibited the LPS induction of TNF-α and nitric oxide synthase-2, but IL-10 suppression of TNF-α and nitric oxide synthase-2 was reduced markedly by *Hmox1* RNA silencing (Fig. 2*C*). The same result was obtained in J774.1 cells (Fig. 2*D*), indicating that HO-1/CO is required for IL-10 to inhibit the LPS response.

sIL-1Ra Gene and Protein Expression—In macrophages, IL-10 is associated with the anti-inflammatory molecule sIL-

1Ra (15), which could also connect counter-inflammation to mitochondrial biogenesis. We assessed hepatic sIL-1Ra mRNA levels in mice 24 h after CO exposure (250 or 500 ppm for 1 h) and demonstrated a pattern of induction similar to that of IL-10 (Fig. 3*A*). In the liver (90), sIL-1Ra protein levels after CO exposure corroborated the mRNA data; the protein increased significantly compared with controls (Fig. 3*A*).

In HepG2 and in J774.1 cells, sIL-1Ra protein increased in response to LPS and to DCM/CO with a greater effect of LPS in J774.1 cells and DCM/CO in HepG2 cells (Fig. 3, *B* and *C*). The use of both agents had additive effects in both cell lines. *Hmox1* or *Nfe2l2* RNA silencing diminished the sIL-1Ra responses to the stimuli equally (Fig. 3, *B* and *C*). These results imply that CO and LPS elicit anti-inflammatory cytokine expression through multiple and overlapping but not identical transcriptional elements.

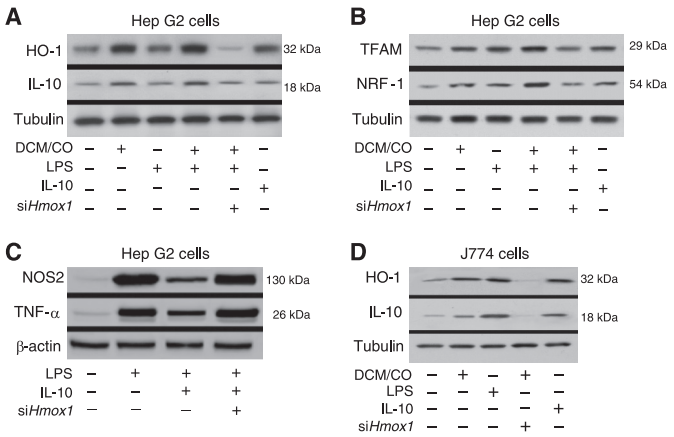

FIGURE 2. ***Hmox1* RNA silencing in HepG2 and J774.1 cells blocks IL-10 expression and counter-inflammatory activity.** *A*, HepG2 cells treated with DCM/CO or LPS for 6 h show HO-1 and IL-10 up-regulation at 24 h. CO + LPS promotes HO-1 and IL-10 expression. *Hmox1* silencing blocks the effect of CO + LPS on IL-10 expression, and incubation with IL-10 increases HO-1 protein levels. *B*, HepG2 cells stimulated with DCM/CO, LPS, or both show TFAM and NRF-1 up-regulation at 24 h. *Hmox1* RNA silencing blocks TFAM and NRF-1 induction by CO + LPS. *C*, LPS-stimulated TNF-α and nitric oxide synthase-2 (*NOS2*) induction in HepG2 cells is inhibited by IL-10 (10 ng/ml), but suppression of TNF-α and nitric oxide synthase-2 by IL-10 is inhibited by si*Hmox1*. *D*, murine J774.1 macrophages show HO-1 and IL-10 induction after DCM/CO and after LPS challenge. IL-10 induces HO-1 within 6 h and to full effect by 24 h. *Hmox1* silencing blocks the DCM/CO effect on IL-10.

HO-1/CO and Co-activation of Mitochondrial Biogenesis and Anti-inflammation—A common induction pattern for IL-10 transcription and mitochondrial biogenesis by CO and LPS raised the prospect of a common regulatory pathway, for instance through Nfe2l2 (Nrf2) signaling (42), which increases both HO-1 (48) and IL-10 expression. We used multiple approaches to examine the role of Nfe2l2 as well as other transcriptional regulators of mitochondrial biogenesis in *IL10* and *IL1Ra* gene regulation.

A computer analysis of the human and mouse promoters using MatInspector and the TRANSFAC database (Genomatix Software) detected putative binding sites for Nfe2l2 and at least three other relevant transcription factors: NRF-1, nuclear respiratory factor-2 (NRF-2), and MEF2. We aligned the *IL10* promoter sequences with DNA Block Aligner (DNAsis software) to identify species-conserved regions that are most likely to represent functional elements (supplemental Fig. S1*A*). Putative binding sites for Nfe2l2, NRF-2 (Gabpa), and MEF2 were identified in the first 500 bp after the TATA box with >90% canonical consensus and >85% conservation scores. Using the same stringency, we identified putative binding sites on the *IL1Ra* promoter for NRF-1 and MEF2 (supplemental Fig. S1*B*). MEF2 has been associated with IL-10 expression, but HO-1/CO is not known to activate *MEF2* genes. In the liver, MEF2A and -2D regulate cell activity and growth, *e.g.* in stellate cells (49), and *MEF2A* is a target of NRF-1, which is activated by HO-1/CO (50).

Nuclear Nfe2l2, MEF2, and NRF-2—Although HO-1/CO activates Nfe2l2 (51), nothing addresses whether IL-10 expression depends on the other transcription factors. Preliminary studies indicated that hepatic nuclear Nfe2l2, MEF2, and NRF-2α (Gabpa) protein increase after CO breathing in mice; 1 h of CO increased all three nuclear proteins by 6 h (Fig. 4*A*). The peak effect was at 250 ppm, which we used subsequently.

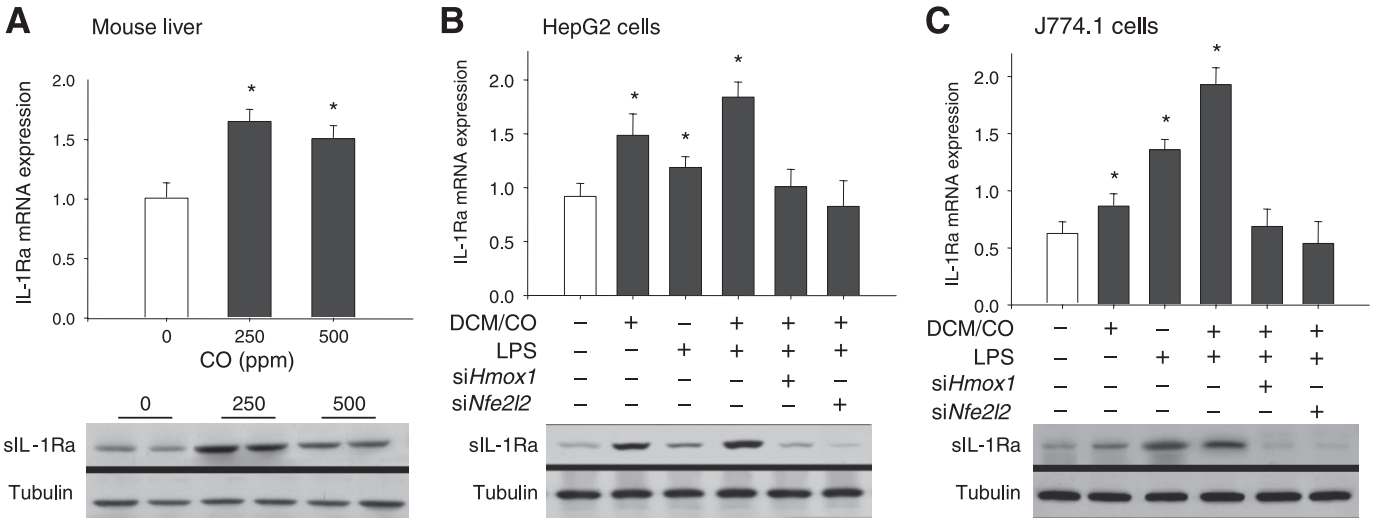

FIGURE 3. **HO-1/CO and LPS-induced *sIL1Ra* gene expression.** *A*, C57BL/6 mouse hepatic sIL-1Ra mRNA and protein levels measured by quantitative RT-PCR and by Western analysis 24 h after 1 h of CO (250 or 500 ppm). *B*, HepG2 cell sIL-1Ra mRNA and protein levels after DCM/CO, LPS, or both. RNA silencing of *Hmox1* or *Nfe2l2* blocks up-regulation of mRNA and protein. *C*, in J774.1 macrophages, sIL-1Ra mRNA and protein expression increase after LPS and DCM/CO or both. IL-1Ra mRNA and protein levels are decreased by si*Hmox1* or by si*Nfe2l2*. *, $p < 0.05$ *versus* control values for $n = 3$ studies.

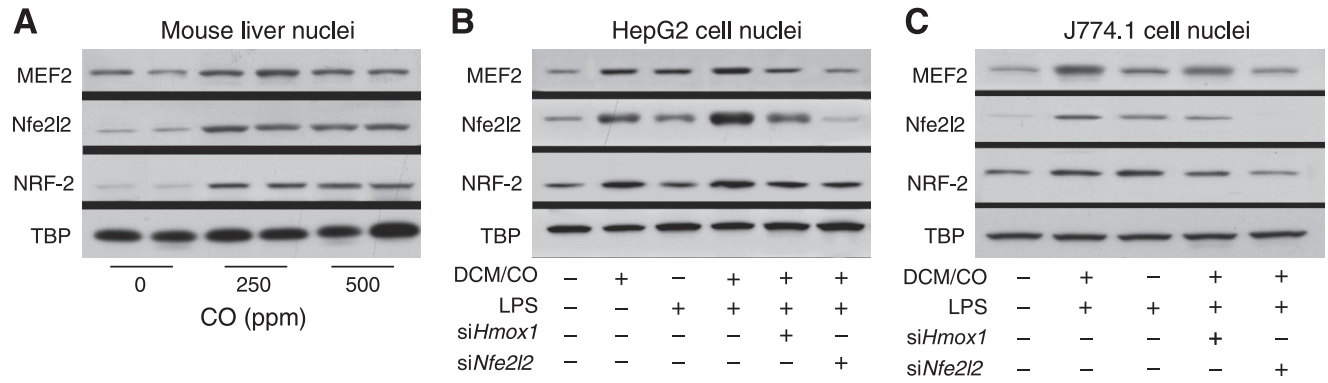

FIGURE 4. **Nuclear MEF2, Nfe2l2, and NRF-2 (Gabpa) protein levels in mouse liver and HepG2 and J774.1 cells.** These nuclear protein levels were checked in mouse liver after CO and in both cell lines after DCM/CO exposure. *A*, 1 h of CO breathing in mice increased hepatic MEF2, Nfe2l2, and NRF-2 nuclear protein relative to TATA-binding protein (*TBP*). *B*, in HepG2 cells, DCM/CO and LPS each increased nuclear MEF2, Nfe2l2, and NRF-2 protein levels, and the DCM/CO + LPS combination enhanced the effects. *Hmox1* RNA silencing decreased nuclear MEF2, Nfe2l2 and NRF-2 protein levels, whereas Nfe2l2 silencing sharply decreased nuclear MEF2 and modestly decreased nuclear NRF-2. *C*, changes in J774.1 cell nuclear protein levels after DCM/CO and LPS and after si*Hmox1* or si*Nfe2l2* were similar to those for Hep2G cells for all three proteins.

In HepG2 cells, DCM/CO also increased nuclear MEF2, Nfe2l2, and NRF-2 levels and was additive to the LPS effect (Fig. 4*B*). *Hmox1* RNA silencing decreased nuclear Nfe2l2 and NRF-2 levels but only modestly decreased nuclear MEF2 levels (Fig. 4*B*). *Nfe2l2* RNA silencing, however, sharply decreased nuclear MEF2 and slightly decreased NRF-2 levels (Fig. 4*B*). In J774.1 macrophages, *Hmox1* silencing had a smaller effect than in HepG2 cells, whereas *Nfe2l2* silencing had a similar effect in both cell lines (Fig. 4*C*). Replicate studies confirmed that *Nfe2l2* silencing produced more attenuation of nuclear MEF and NRF-2 accumulation than did *Hmox1* silencing.

Mitochondrial Biogenesis Transcription Factor Recruitment to IL10 and IL1Ra—Transcription factor binding activities were measured in nuclear extracts of HepG2 cells for the Nfe2l2 and MEF2 sequences on the human *IL10* promoter. These assays showed increased binding activity for both transcription factors after DCM/CO exposure (Fig. 5, *A* and *B*). The LPS-stimulated binding activity for both proteins was comparatively modest; by implication, LPS induction of IL-10 involves not only HO-1, but also other elements, *e.g.* NF-κB.

Nfe2l2 and MEF2A nuclear translocation depends on phosphorylation, which is regulated, for instance, by Akt/PKB and p38 MAPK. NRF-1 translocation is also regulated by Akt/PKB. We evaluated the influence of p38 and Akt on the CO response in HepG2 cells with inhibition of p38 (SB203580; SB20) or PI-3K/Akt (LY294002; LY29). Activation of Nfe2l2 by DCM/CO was partly blocked by p38 inhibition, but fully abrogated by Akt inhibition. The effect of DCM/CO on MEF2 activation was blocked by inhibiting either kinase (Fig. 5, *A* and *B*).

To determine how HO-1/CO promotes IL-10 transcription, we generated cross-linked nuclear lysates from HepG2 cells after a 60-min exposure to DCM/CO, LPS, or both. Sequential ChIP assay (ChIP-ReChIP) was performed on genomic DNA with anti-RNA polymerase II or with control IgG (data not shown) and probed for interactions with Nfe2l2, MEF2, and NRF-2 (Gabpa) at the human *IL10* promoter. In control nuclei, almost no polymerase II signal was detected at the *IL10* promoter, but the signal was increased by DCM/CO and LPS (Fig. 5*C*). The largest increases occurred after LPS + DCM/CO consistent with the changes in IL-10 mRNA expression.

Chromatin IP assays were performed to evaluate *IL10* promoter binding to MEF2, Nfe2l2, and NRF-2 using validated antibodies and primer sets for these sites. We also checked the *IL1Ra* promoter for NRF-1 and MEF2 binding at our predicted binding sites. *IL10* promoter DNA did not co-precipitate with control IgG (Fig. 5*D*). ChIP assays for Nfe2l2 detected no transcription factor binding at the *IL10* promoter in control or LPS-stimulated cells, but Nfe2l2 binding was detectable after DCM/CO (Fig. 5*D*). MEF2 and NRF-2 occupancy was minimal in control HepG2 nuclei, after DCM/CO and LPS, both factors were bound, and DCM +LPS produced stronger binding (Fig. 5*D*). *IL1Ra* promoter DNA did not precipitate with control IgG, and nonstimulated nuclei showed no MEF2 or NRF-1 binding, but both transcription factors bound after DCM/CO and after LPS, and the combination produced strong occupancy (Fig. 5*D*). In mouse liver nuclei, we found CO-dependent Nfe2l2, MEF2, and NRF-2 recruitment to the *IL10* promoter (Fig. 5*E*). These data correlated with the changes in IL-10 mRNA and protein in the liver.

MEF2 Expression and Nuclear Translocation in HepG2 Cells—We used confocal microscopy to evaluate MEF2 nuclear localization in HepG2 cells treated with LPS and/or DCM/CO. *Nfe2l2* RNA silencing was used to evaluate the DCM/CO effect on MEF2, whereas *NRF1* silencing was used to check *MEF2* regulation. The effectiveness of *Nfe2l2* silencing is shown by Western blot, where Nfe2l2 protein decreases by ~80% at 48 h (Fig. 6*A*). Fig. 6*B* indicates that NRF-1 protein increases after DCM/CO, and after *NRF1* RNA silencing, the loss in MEF2 signal at 24 h is comparable to that of *Nfe2l2* silencing.

HO-1 distribution was checked in HepG2 cells pre- and post-DCM/CO and LPS treatment by fluorescence techniques. In control cells, HO-1 was restricted to the cytoplasm (Fig. 6*C*, *panels A–C*, *green*), and nuclear MEF2 was not detectable. However, after a 1-h DCM/CO exposure, MEF2 had accumulated in the nucleus by 2 h (Fig. 6*C*, *panels D–F*, *red*) and dissipated by 6 h (data not shown). Similarly, 2 h after LPS, HO-1 expression was abundant, and nuclear MEF2 levels increased sharply (Fig. 6*C*, *G–I*) and disappeared by 6 h (data not shown). Nfe2l2-silenced cells after DCM/CO still showed abundant HO-1 staining, but nuclear MEF2 was undetectable (Fig. 6*C*,

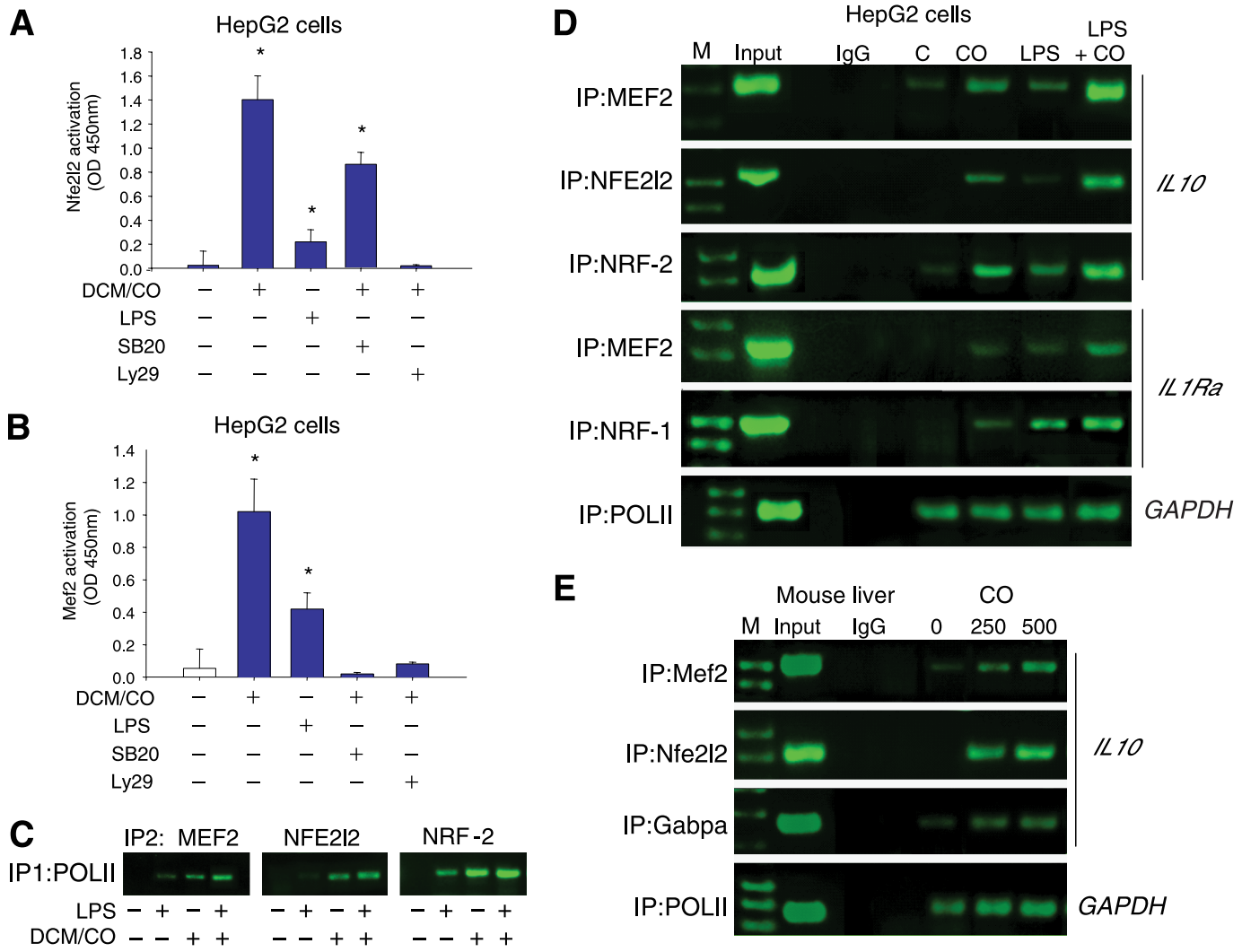

FIGURE 5. **Nuclear Nfe2l2 and MEF2 transcription factor binding activity after HO-1 induction in cells.** Binding activity in HepG2 cell nuclear extracts for Nfe2l2 (*A*) and MEF2 (*B*) after DCM/CO or LPS. Both exposures activate these transcription factors, but DCM/CO is more pronounced. The ability of DCM/CO to activate Nfe2l2 is partially blocked by p38 MAPK inhibition (SB20) and fully blocked by Akt inhibition (LY29), whereas either inhibitor blocks MEF2 activation by DCM/CO. The histograms represent means ± S.E. of duplicates in three experiments. *, $p < 0.05$ compared with control cells. *C*, sequential ChIP assay (ChIP-ReChIP) was performed on HepG2 cell genomic DNA with anti-RNA polymerase II (*POL II*) or with control IgG (not shown) and probed for interactions with Nfe2l2, MEF2, and NRF-2 at the human *IL10* promoter. DCM/CO (and to a lesser extent LPS) recruits RNA polymerase II to MEF2, Nfe2l2, and NRF-2 binding sites on the *IL10* promoter. *D*, ChIP assay of HepG2 cell nuclei pre- and post-DCM/CO (100 μm) or LPS (15 ng/ml) treatments. PCR was conducted with primer sets for the human *IL10* or the *IL1Ra* promoter regions of interest. LPS and DCM/CO induced MEF2, Nfe2l2, and NRF-2 recruitment to *IL10* promoter and MEF2 and NRF-1 to the *IL1Ra* promoter. *Input* lanes show PCR product derived from chromatin before immunoprecipitation (*IP*) to verify equal loading. GAPDH is a positive control. *E*, ChIP assay of the *Il10* promoter using mouse liver genomic DNA and antibodies for MEF2, Nfe2l2, and NRF-2α (Gabpa). The *Il10* promoter DNA did not co-precipitate with control IgG antibody. Nfe2l2 binding was not detectable at the *Il10* promoter at basal conditions or after LPS but was detectable after CO exposure. MEF2 and Gabpa binding were weakly detected at the basal state but strongly recruited to the *Il10* promoter after CO exposure.

J–L). This result indicates that HO-1/CO is upstream of Nfe2l2, which is required for the expression and nuclear localization of MEF2.

*NF-k*B *and Related Signals*—Because LPS activates both anti- and proinflammatory cytokines, we checked HepG2 cells for a role of NF-kB in the LPS + DCM/CO response using the structurally-unrelated inhibitors, SN-50 and PDTC (supplemental Fig. S2, *A* and *B*). Neither SN-50 nor PDTC prevented LPS-induced IL-10 induction, but DCM/CO was effective in decreasing the TNF-α production. Based on the role of PI-3K/Akt in translocation of mitochondrial biogenesis transcription factors, we checked and found that Akt inhibition also blocked CO inhibition of TNF-α production.

In addition, we tested STAT3 for a role in LPS-stimulated HO-1 and IL-10 induction in HepG2 cells using the JSI-24 inhibitor, which decreased HO-1 and IL-10 expression after DCM/CO (supplemental Fig. S2*C*). We also examined p38 MAPK because it may be involved in counter-inflammation (52). Inhibition of p38 with SB20 attenuated HO-1 and IL-10 induction by LPS, whereas HO-1 induction by DCM/CO was largely p38-independent and PI3K/Akt-dependent (supplemental Fig. S2*D*). Hence, we implicate PI-3K/Akt and STAT3 but not NF-kB or p38 in HO-1 and IL-10 regulation in HepG2 cells.

Nfe2l2-regulated Genes—Because *Nfe2l2* is activated by HO-1/CO and Nfe2l2 regulates both *Hmox1* (41) and *NRF1* in

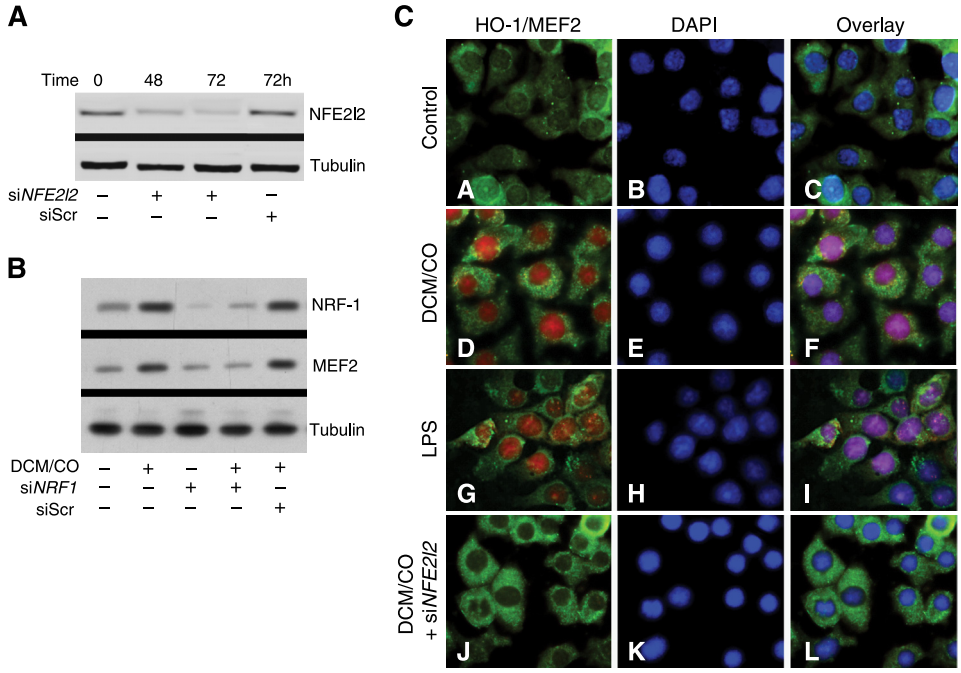

FIGURE 6. **MEF2 regulation and nuclear translocation by Nfe2l2 in HepG2 cells after LPS or DCM/CO exposure.** *A*, Western blot showing that *Nfe2l2*, but not scrambled siRNA decreases Nfe2l2 by >80% at 72 h. *B*, Western blot showing increased NRF-1 protein after DCM/CO and that *NRF1* silencing leads to loss of MEF2 by 24 h. Tubulin is a reference protein. *C*, confocal microscopy in HepG2 cells treated with DCM/CO (100 μm) for 1 h or LPS (15 ng/ml) for 2 h, washed, and incubated for 4 h in fresh media. Some cells were transfected with Nfe2l2 siRNA. Cells were fixed, incubated with primary anti-HO-1 and anti-MEF2, and developed with secondary green Alexa Fluor 488 (HO-1) or red Alexa Fluor 595 (MEF2) antibodies. In control cells, HO-1 was restricted to cytoplasm, and no nuclear MEF2 was detected (*panels A–C*). DCM/CO (1-h exposure) caused robust nuclear MEF2 translocation by 2 h (*panels D–F*). After 2 h of LPS, nuclear MEF2 levels were also increased (*panels G–I*). Cells after si*Nfe2l2* still showed cytoplasmic HO-1 after DCM/CO, but MEF2 did not accumulate in the nuclei (*panels J–L*). Nuclei are stained with DAPI (*blue*), and images for MEF2 were taken at ×600. *Scr*, scrambled.

mitochondrial biogenesis, we confirmed activation of other Nfe2l2-regulated gene promoters having antioxidant response elements (40, 53). Nfe2l2 also activates *NRF1*, and as shown here in the liver and in (54), NRF-1 activates *MEF2*. Nfe2l2 is regulated by transcription and by cytoplasmic Keap1, which promotes degradation of the transcription factor (53). To further evaluate this in HepG2 cells, we performed proteasome and transcription inhibition studies and followed the IL-10 response (Fig. 7). LPS and DCM/CO increased Nfe2l2 protein in the cytoplasmic and nuclear fractions with a nuclear peak by 4 h (Fig. 7*A*) that remained elevated for 24 h (data not shown). Proteasomal inhibition with MG132 further increased nuclear Nfe2l2 (Fig. 7*B*), whereas inhibition of transcription with α-amanitin sharply reduced nuclear Nfe2l2 (Fig. 7*B*). By inference, transcription factor stability and gene transcription are both involved in HO-1/CO anti-inflammatory gene regulation by Nfe2l2. Using DCM/CO to increase Nfe2l2 nuclear translocation in HepG2 cells, we checked *IL10* and *NQO1* activation. DCM/CO increased mRNA levels for both after MG132 (Fig. 7, *C* and *D*), whereas despite MG132 addition, mRNA expression for both was blocked in α-amanitin controls.

Nfe2l2$^{-/-}$ *Mice*—On the basis of the cell data implicating Nfe2l2 in HO-1 induction and in the transcriptional regulation of both anti-inflammatory IL-10 expression and mitochondrial biogenesis, we evaluated and compared the relevant responses of WT and Nfe2l2$^{-/-}$ mice to the implantation of *E. coli*-infected fibrin clots. In this model, at a dose of 10^8 cfu, Nfe2l2$^{-/-}$ mice showed severe early hepatic damage compared with WT mice, *i.e.* more focal hemorrhage and inflammation, ductal dilation, and hepatocyte vacuolization and autolysis (supplemental Fig. S3). Nfe2l2$^{-/-}$ mice also died of *E. coli* sepsis more rapidly than did WT mice (Fig. 8*A*), and consecutive daily treatments with CO (250 ppm for 1 h on days 1–3) rescued WT but not Nfe2l2$^{-/-}$ mice (Fig. 8*A*). This finding highlights the Nfe2l2-dependent survival role for CO in this model.

To avoid selection bias due to early mortality in Nfe2l2$^{-/-}$ mice, we compared activation of hepatic counter-inflammation and mitochondrial biogenesis at 0, 6, and 24 h after 10^7 cfu of *E. coli*. We compared mRNA levels for HO-1 (Fig. 8*B*), NRF-1 (Fig. 8*C*), and a master mitochondrial biogenesis co-activator, PGC-1α (Fig. 8*D*). Nfe2l2$^{-/-}$ mice had substantially lower mRNA levels for all three genes than WT after *E. coli* inoculation. We also compared hepatic TNF-α mRNA with IL-10 mRNA levels and those for two independent anti-inflammatory genes, *Socs3*, and *Bclx*$_L$. In contrast to WT mice, Nfe2l2$^{-/-}$ mice showed greater increases in TNF-α mRNA (Fig. 8*E*) and no responses in IL-10 (Fig. 8*F*), Bcl-x$_L$ (Fig. 8*G*), or Socs3 (Fig. 8*H*) mRNA levels in the 24 h after infection.

DISCUSSION

Mitochondrial biogenesis is linked closely to the preservation of mitochondrial function and to survival in severe sepsis (38, 55), yet few interactions between the mitochondrial biogenesis transcriptional program and inflammatory gene regulation have been identified. In this context, we present the first evidence that regulation of mitochondrial biogenesis generates a simultaneous anti-inflammatory response that protects the

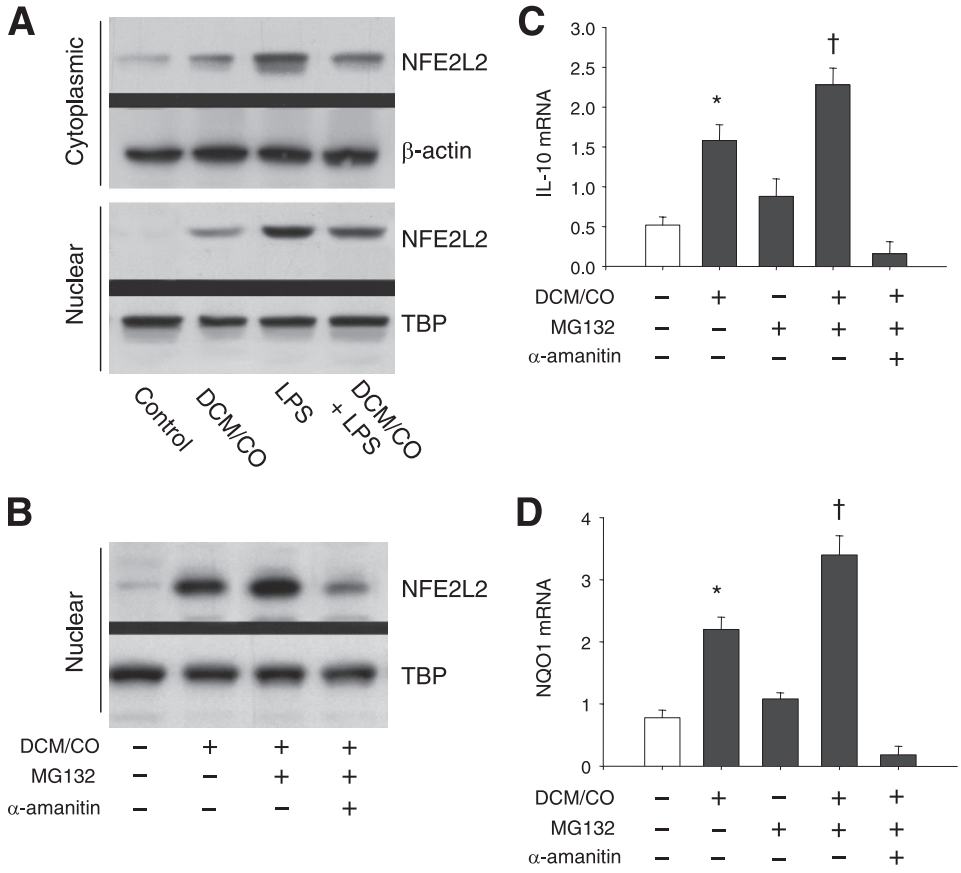

FIGURE 7. **Nuclear and cytoplasmic Nfe2l2 protein in HepG2 cells.** *A*, DCM/CO and LPS increase nuclear and cytoplasmic Nfe2l2 protein levels within 4 h. *TBP*, TATA binding protein. *B*, the MG132 proteasome inhibitor further increased Nfe2l2 nuclear protein at 4 h, whereas inhibition of transcription with α-amanitin leads to a dramatic loss of Nfe2l2 nuclear protein. In *C* and *D*, HepG2 cells were treated with DCM/CO to increase Nfe2l2 nuclear translocation and *IL10* and *NQO1* transcription. MG132 clearly increases mRNA levels for IL-10 (*C*) and NQO1 (*D*) in response to DCM/CO, whereas α-amanitin blocks mRNA expression for both genes. *, $p < 0.05$ *versus* control; †, $p < 0.05$ *versus* control and DCM/CO.

liver, a central organ of LPS responsiveness and LPS tolerance, against lasting inflammatory attack.

Mitochondrial biogenesis is activated in sepsis by mitochondrial oxidant damage (39), by nitric oxide (56), and by the classical NF-kB pathway, for instance, in the liver (46). In general, acute inflammation also induces HO-1 (24), which stimulates both anti-inflammatory IL-10 synthesis (16) and mitochondrial biogenesis (30). These independent observations led us to propose that the transcriptional program of mitochondrial biogenesis harbors a protective counter-inflammatory function through HO-1 that limits proinflammatory cytokine synthesis.

Apart from the HO-1 association with IL-10 induction, nothing has been known about the interaction mechanism and little about how the molecules help resolve tissue damage (57). Free heme is cytotoxic, and heme clearance reduces oxidative stress and apoptosis (58), which is assumed to promote resolution of inflammation. IL-10 attenuates the host response to microbial antigens, to cytokines and chemokines (21, 59), to ischemia reperfusion, and to some drug-induced injuries (13, 60). This limits tissue damage, but the persistence of IL-10 leads to immune suppression and to impaired pathogen clearance in infection (61). Moreover, nothing has been known about whether HO-1/CO is connected to other anti-inflammatory effectors, such as IL-1Ra.

We have provided multiple lines of evidence in human and mouse cells of a role for HO-1 in transcriptional co-activation of mitochondrial biogenesis and anti-inflammation. First, HO-1 is necessary for IL-10 production by LPS, and *Hmox1*-silenced cells do not show IL-10-mediated suppression of LPS-induced TNF-α and nitric oxide synthase-2 production. HO-1 has anti-inflammatory and anti-apoptotic effects involving p38, for example in endothelial cells (62), also seen here in human hepatocytes and mouse macrophages after LPS. CO suppresses TNF-α production by activating PI3K/Akt, which also supports nuclear Nfe2l2 and MEF2 translocation in their roles in mitochondrial biogenesis (30, 63).

Second, the proximal *IL10* promoter region contains binding sites that by ChIP are active for three transcription factors that regulate mitochondrial biogenesis: Nfe2l2, NRF-2 (Gabpa), and MEF2. Nfe2l2 and NRF-2 are activated by HO-1/CO, whereas MEF2 is activated by NRF-1 (54). All four transcription factors stimulate mitochondrial biogenesis; MEF2A for instance, increases PGC-1α co-activator expression (50), whereas NRF-1, under redox regulation by Nfe2l2 (30), is integral to the expression of mitochondrial transcriptome genes (64).

A third aspect involves the IL-1 receptor antagonist, sIL-1Ra, which is synthesized after LPS challenge and shown here to be regulated by HO-1/CO. This endogenous receptor antagonist

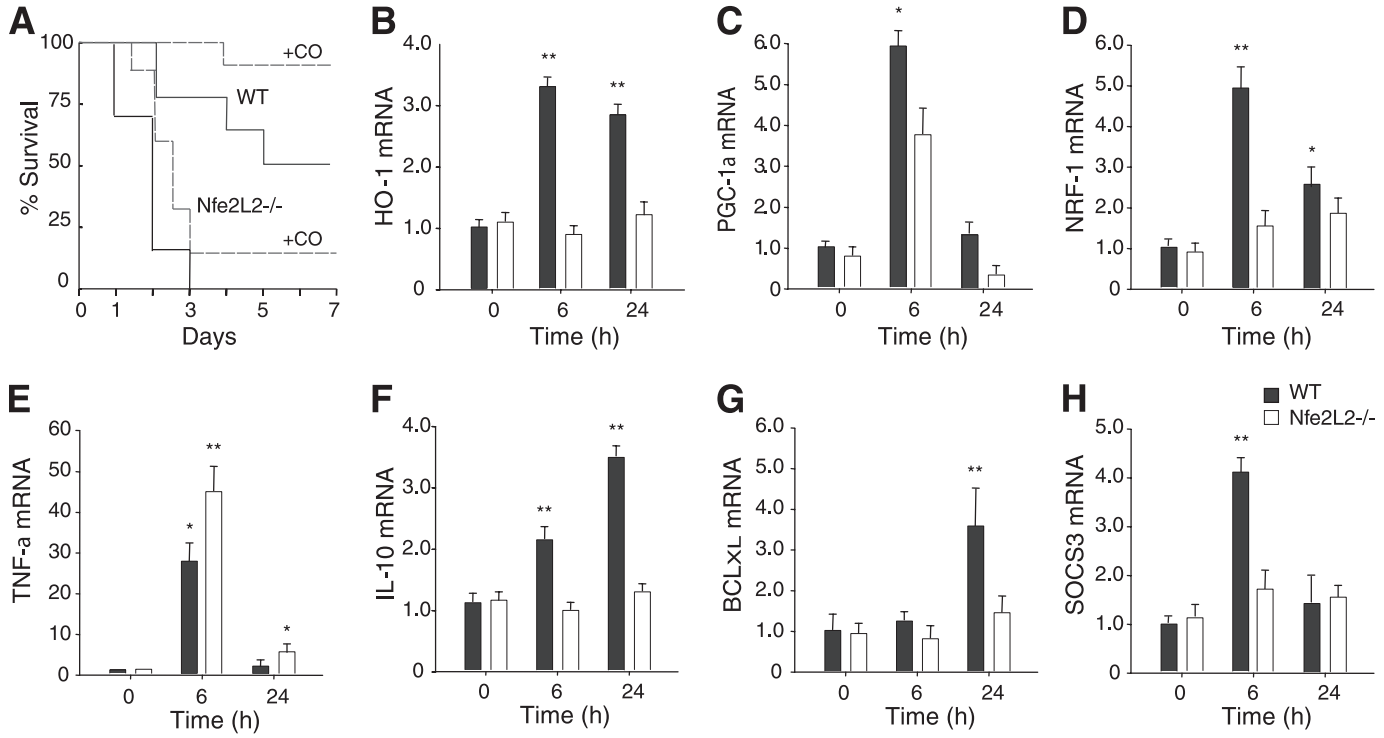

FIGURE 8. ***E. coli* sepsis in wild-type and Nfe2l2$^{-/-}$ mice.** *A*, increased early mortality in Nfe2l2$^{-/-}$ mice after peritoneal implantation of 10^8 cfu *E. coli*-containing fibrin clots compared with C57BL/6 (WT) mice ($p < 0.05$ by Chi square). CO therapy (250 ppm for 1 h/day on days 1–3) rescues WT but not Nefel2$^{-/-}$ mice (*red lines*). *B*, after 10^7 cfu *E. coli*, hepatic *Hmox1* mRNA levels increase in WT but not Nfe2l2$^{-/-}$ mice 6 and 24 h after infection. For activation of mitochondrial biogenesis, NRF-1 mRNA is shown in *C*, and PGC-1α co-activator mRNA is shown in *D*. Compared with WT mice, Nfe2l2$^{-/-}$ mice also show significantly greater increases in TNF-α mRNA levels (*E*) and no responses in IL-10 (*F*), Bcl-x_L (*G*), or Socs3 (*H*) mRNA over 24 h post-infection. **, $p < 0.05$ *versus* 0 h control values and *versus* null strain; *, $p < 0.05$ *versus* 0 h control values ($n = 3$–4 mice per group at each time).

prevents deleterious downstream responses to IL-1α and 1β; moreover, *IL1Ra* gene expression in HepG2 cells is blocked by *Hmox1* or by *Nfe2l2* silencing, and by ChIP, the *IL1Ra* promoter binds NRF-1 and MEF2.

Fourth, Nfe2l2-silenced cells challenged with LPS do not generate IL-10 or IL-1Ra, but produce more TNF-α, which increases mitochondrial injury (65), intrinsic apoptosis (66), and reactive oxygen species-induced organ damage (67). TNF-α is in important pathologically as shown by the efficacy of anti-TNF therapy in several human inflammatory diseases (68).

Lastly, mice with genetic loss of *Nfe2l2* were studied with endpoints selected on the basis of the cell data and the literature to demonstrate that this protective system operates during *E. coli* sepsis. The lack of *Nfe2l2* in sepsis greatly increases liver damage and lethality through loss of *Hmox1* expression and enhancement of TNF-α levels. Moreover, *Nfe2l2*$^{-/-}$ mice show impaired NRF-1 and PGC-1α gene activation and fail to increase anti-inflammatory IL-10, Socs3, or Bcl_{XL} expression in the *E. coli* model. Lack of Bcl_{XL} expression increases the risk of intrinsic apoptosis (69) but also suppresses caspase-1-dependent IL-1β processing by interaction with NALD1 (70). Furthermore, low dose CO, similar to other cell-protective CO therapy (71), improves survival in the sepsis model in WT, but not Nfe2l2-deficient mice. Collectively, these data support that Nfe2l2 transcriptional control of mitochondrial biogenesis is coupled to hepatic counter-inflammation in the response to Gram-negative infection.

The transcriptional co-regulation of mitochondrial biogenesis and counter-inflammation through *IL10* and *IL1Ra* promotes cell survival by suppressing TNF-α production and perhaps other NF-κB proinflammatory cytokines, *e.g.* through autocrine suppressors of TNF-α and MHC class II antigen production. IL-10 is also a macrophage and B lymphocyte survival factor; for instance, in J774.1 mouse macrophages, IL-10 upregulates some 50 stress-response and immunoregulatory genes (72). Apart from IL-10, HO-1/CO also has pleiotropic effects in monocytes and may exert some control over NF-kB target gene selectivity (27).

Endogenous CO generates an oxidant effect by increasing mitochondrial H_2O_2 production, which promotes mitochondrial biogenesis (63), in part by Keap1 oxidation and Nfe2l2 nuclear translocation (73, 74). Nfe2l2 activates the xenobiotic defenses, glutathione synthesis (75), superoxide detoxification (42), and *NRF1* (30). CO activates Akt/PKB, which inhibits caspase-dependent apoptosis (76), but also facilitates Nfe2l2 and NRF-1 nuclear translocation and hence mitochondrial biogenesis (30, 47).

The present work adds at least two major anti-inflammatory genes, *IL10* and *IL1Ra*, to the transcriptional network of mitochondrial biogenesis. These molecules respectively limit NF-κB-dependent mediator production and dampen IL-1β and IL-1α effector functions in sepsis (5, 77, 78). Furthermore, IL-1β maturation and release is controlled by the NLRP3 inflammasome and involves caspase-1 activation (79), which is modulated by Bcl_{XL} (80).

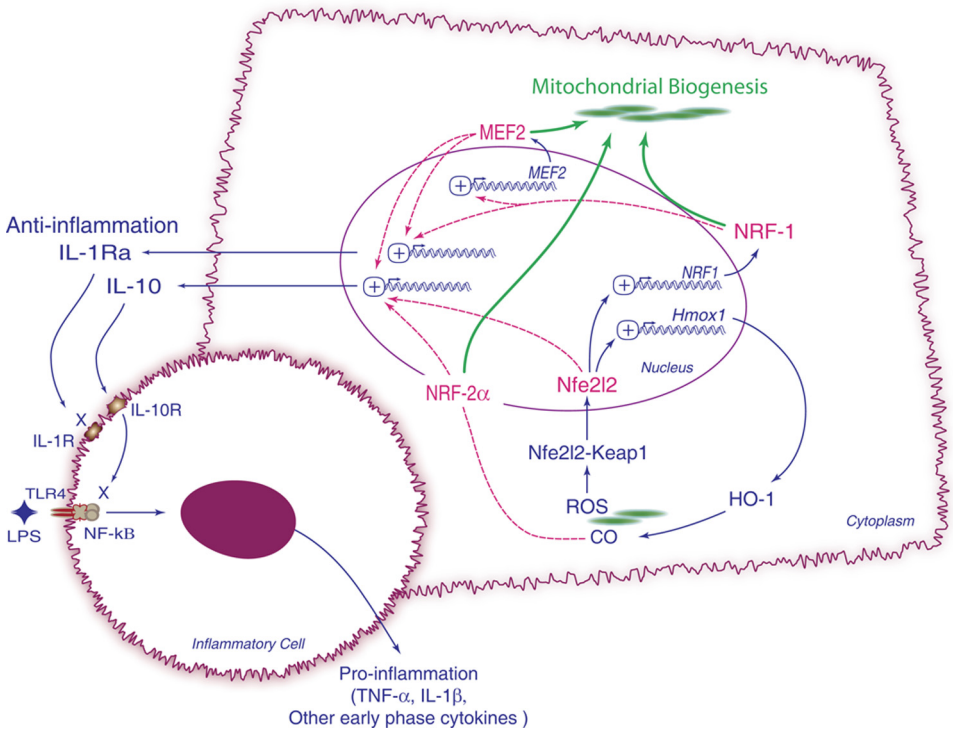

FIGURE 9. **Working diagram of the HO-1/CO system and *IL10* and *IL1Ra* activation during mitochondrial biogenesis.** The two-cell model indicates the transcriptional integration of *IL10* and *IL1Ra* gene expression with mitochondrial biogenesis through a redox-regulated cycle involving HO-1 and Nfe2l2. Nfe2l2 is involved both in *Hmox1* activation and in the activation of *NRF1* and *IL10*. NRF-1 activates *MEF2* and *IL1Ra*, and MEF2 activates *IL10*. HO-1 activates NRF-2 (Gabpa) by an unknown mechanism that also contributes to *IL10* activation. The transcription factors involved in mitochondrial biogenesis and anti-inflammation are highlighted in *red*. Activation of counter-inflammatory genes blocks the LPS/ Toll-like receptor 4 (*TLR4*)-dependent early-phase proinflammatory response mediated by TNF-α and IL-1β.

The importance of IL-10 is also illustrated by its prognostic value in the critically ill. IL-10 administration reduces proinflammatory cytokine levels (81) and blocks monocyte activation (82), whereas endogenous plasma IL-10 relates to outcome in septic patients. Promoter polymorphisms for low IL-10 production predict higher death rates in severe sepsis (83), whereas HIV patients with polymorphisms for high IL-10 more often progress to AIDS (84). Chronic liver failure patients also show persistently high plasma IL-10 levels and often have prolonged sepsis (7).

A working diagram of the Nfe2l2/HO-1/CO regulation of *IL10* and *IL1Ra* in the setting of mitochondrial biogenesis is provided in Fig. 9. The diagram highlights the HO-1 links to Nfe2l2, IL-10, and sIL1Ra, emphasizing a transcriptional network supported by the data. There are still unknowns in this network; for instance, HO-1/CO-mediated activation of NRF-2α (Gabpa) operates by an unknown mechanism. Fig. 9 also simplifies Nfe2l2-Keap1 signaling, omits IL-10 regulation by interferon (85) and by glucocorticoids (86), and ignores interactions of MEF2 with PGC-1α and class 2 histone deacetylases (87) or cAMP response element (CRE) binding/activating transcription factor (CREB/ATF) sites (88, 89). CREB is regulated in part by NO and by metabolic demand and co-activates *NRF1* after LPS (46).

Lastly, computer predictions of promoter binding sites for these four transcription factors in the anti-inflammatory genes of interest reveals many more sites than are found in the main NF-κB-dependent proinflammatory genes, including *TNFα* and *IL1β*. This is shown simply by the relative abundance of potential 5′-DNA binding sites for each transcription factor for the two groups of human genes (supplemental Table 1).

In conclusion, the nuclear transcriptional program of mitochondrial biogenesis, under redox regulation by HO-1/CO and Nfe2l2, increases the expression of two major anti-inflammatory genes, *IL10* and *IL1Ra*. By implication, the activation of mitochondrial biogenesis synchronously up-regulates counter-inflammation, thereby limiting inflammatory damage to the organelles that would impact negatively on cell function and survival during bacterial infection. This network operates in conjunction with cellular antioxidant and xenobiotic defenses to optimize cell protection by curtailing inflammation and oxidative stress while restoring the capacity for energy production. However, persistent IL-10 and sIL-1Ra synthesis during frequent cycles of mitochondrial damage and repair would be immunosuppressive, and by inference contribute to the observed high prevalence of secondary infection in sepsis.

Acknowledgments—We thank Craig Marshall, John Patterson, Kathy Stempel, Lynn Tatro, and Martha Salinas for excellent technical assistance.

REFERENCES

1. Rittirsch, D., Flierl, M. A., and Ward, P. A. (2008) *Nat. Rev. Immunol.* **8,** 776–787
2. Hotchkiss, R. S., and Opal, S. (2010) *N. Engl. J. Med.* **363,** 87–89
3. Winters, B. D., Eberlein, M., Leung, J., Needham, D. M., Pronovost, P. J., and Sevransky, J. E. (2010) *Crit. Care Med.* **38,** 1276–1283
4. Knolle, P., Schlaak, J., Uhrig, A., Kempf, P., Meyer zum Büschenfelde,

K. H., and Gerken, G. (1995) *J. Hepatol.* **22,** 226–229
5. Dinarello, C. A. (2009) *Annu. Rev. Immunol.* **27,** 519–550
6. Madan, R., Demircik, F., Surianarayanan, S., Allen, J. L., Divanovic, S., Trompette, A., Yogev, N., Gu, Y., Khodoun, M., Hildeman, D., Boespflug, N., Fogolin, M. B., Gröbe, L., Greweling, M., Finkelman, F. D., Cardin, R., Mohrs, M., Müller, W., Waisman, A., Roers, A., and Karp, C. L. (2009) *J. Immunol.* **183,** 2312–2320
7. Lin, C. Y., Tsai, I. F., Ho, Y. P., Huang, C. T., Lin, Y. C., Lin, C. J., Tseng, S. C., Lin, W. P., Chen, W. T., and Sheen, I. S. (2007) *J. Hepatol.* **46,** 816–826
8. Palmer, D. C., and Restifo, N. P. (2009) *Trends Immunol.* **30,** 592–602
9. Saraiva, M., and O'Garra, A. (2010) *Nat. Rev. Immunol.* **10,** 170–181
10. Mosser, D. M., and Zhang, X. (2008) *Immunol. Rev.* **226,** 205–218
11. Rai, R. M., Loffreda, S., Karp, C. L., Yang, S. Q., Lin, H. Z., and Diehl, A. M. (1997) *Hepatology* **25,** 889–895
12. Wang, S. C., Ohata, M., Schrum, L., Rippe, R. A., and Tsukamoto, H. (1998) *J. Biol. Chem.* **273,** 302–308
13. Bourdi, M., Masubuchi, Y., Reilly, T. P., Amouzadeh, H. R., Martin, J. L., George, J. W., Shah, A. G., and Pohl, L. R. (2002) *Hepatology* **35,** 289–298
14. Menezes, G. B., Lee, W. Y., Zhou, H., Waterhouse, C. C., Cara, D. C., and Kubes, P. (2009) *J. Immunol.* **183,** 7557–7568
15. Lai, C. F., Ripperger, J., Morella, K. K., Jurlander, J., Hawley, T. S., Carson, W. E., Kordula, T., Caligiuri, M. A., Hawley, R. G., Fey, G. H., and Baumann, H. (1996) *J. Biol. Chem.* **271,** 13968–13975
16. Lee, T. S., and Chau, L. Y. (2002) *Nat. Med.* **8,** 240–246
17. Mosser, D. M. (2003) *J. Leukoc. Biol.* **73,** 209–212
18. Siewe, L., Bollati-Fogolin, M., Wickenhauser, C., Krieg, T., Müller, W., and Roers, A. (2006) *Eur. J. Immunol.* **36,** 3248–3255
19. Standiford, T. J., Strieter, R. M., Lukacs, N. W., and Kunkel, S. L. (1995) *J. Immunol.* **155,** 2222–2229
20. Berg, D. J., Kühn, R., Rajewsky, K., Müller, W., Menon, S., Davidson, N., Grünig, G., and Rennick, D. (1995) *J. Clin. Invest.* **96,** 2339–2347
21. van der Poll, T., Marchant, A., Buurman, W. A., Berman, L., Keogh, C. V., Lazarus, D. D., Nguyen, L., Goldman, M., Moldawer, L. L., and Lowry, S. F. (1995) *J. Immunol.* **155,** 5397–5401
22. Gérard, C., Bruyns, C., Marchant, A., Abramowicz, D., Vandenabeele, P., Delvaux, A., Fiers, W., Goldman, M., and Velu, T. (1993) *J. Exp. Med.* **177,** 547–550
23. Howard, M., Muchamuel, T., Andrade, S., and Menon, S. (1993) *J. Exp. Med.* **177,** 1205–1208
24. Maines, M. D. (2005) *Antioxid. Redox Signal* **7,** 1761–1766
25. Otterbein, L. E., Soares, M. P., Yamashita, K., and Bach, F. H. (2003) *Trends Immunol.* **24,** 449–455
26. Yao, P., Hao, L., Nussler, N., Lehmann, A., Song, F., Zhao, J., Neuhaus, P., Liu, L., and Nussler, A. (2009) *Am. J. Physiol. Gastrointest. Liver Physiol.* **296,** G1318–1323
27. Chhikara, M., Wang, S., Kern, S. J., Ferreyra, G. A., Barb, J. J., Munson, P. J., and Danner, R. L. (2009) *PLoS One* **4,** e8139
28. Drechsler, Y., Dolganiuc, A., Norkina, O., Romics, L., Li, W., Kodys, K., Bach, F. H., Mandrekar, P., and Szabo, G. (2006) *J. Immunol.* **177,** 2592–2600
29. Mandal, P., Park, P. H., McMullen, M. R., Pratt, B. T., and Nagy, L. E. (2010) *Hepatology* **51,** 1420–1429
30. Piantadosi, C. A., Carraway, M. S., Babiker, A., and Suliman, H. B. (2008) *Circ. Res.* **103,** 1232–1240
31. Kantrow, S. P., Taylor, D. E., Carraway, M. S., and Piantadosi, C. A. (1997) *Arch Biochem. Biophys* **345,** 278–288
32. Brealey, D., Brand, M., Hargreaves, I., Heales, S., Land, J., Smolenski, R., Davies, N. A., Cooper, C. E., and Singer, M. (2002) *Lancet* **360,** 219–223
33. Crouser, E. D., Julian, M. W., Huff, J. E., Struck, J., and Cook, C. H. (2006) *Crit. Care Med.* **34,** 2439–2446
34. Singer, M. (2007) *Crit. Care Med.* **35,** S441–448
35. Suliman, H. B., Carraway, M. S., and Piantadosi, C. A. (2003) *Am. J. Respir. Crit. Care Med.* **167,** 570–579
36. Suliman, H. B., Carraway, M. S., Welty-Wolf, K. E., Whorton, A. R., and Piantadosi, C. A. (2003) *J. Biol. Chem.* **278,** 41510–41518
37. Suliman, H. B., Welty-Wolf, K. E., Carraway, M. S., Schwartz, D. A., Hollingsworth, J. W., and Piantadosi, C. A. (2005) *Faseb J.* **19,** 1531–1533
38. Haden, D. W., Suliman, H. B., Carraway, M. S., Welty-Wolf, K. E., Ali, A. S., Shitara, H., Yonekawa, H., and Piantadosi, C. A. (2007) *Am. J. Respir. Crit. Care Med.* **176,** 768–777
39. Suliman, H. B., Welty-Wolf, K. E., Carraway, M., Tatro, L., and Piantadosi, C. A. (2004) *Cardiovasc. Res.* **64,** 279–288
40. Kensler, T. W., Wakabayashi, N., and Biswal, S. (2007) *Annu. Rev. Pharmacol. Toxicol.* **47,** 89–116
41. Alam, J., Stewart, D., Touchard, C., Boinapally, S., Choi, A. M., and Cook, J. L. (1999) *J. Biol. Chem.* **274,** 26071–26078
42. Suliman, H. B., Carraway, M. S., Ali, A. S., Reynolds, C. M., Welty-Wolf, K. E., and Piantadosi, C. A. (2007) *J. Clin. Invest.* **117,** 3730–3741
43. Suliman, H. B., Babiker, A., Withers, C. M., Sweeney, T. E., Carraway, M. S., Tatro, L. G., Bartz, R. R., Welty-Wolf, K. E., and Piantadosi, C. A. (2010) *Free Radic. Biol. Med.* **48,** 736–746
44. Loots, G. G., and Ovcharenko, I. (2004) *Nucleic Acids Res.* **32,** W217–221
45. Loots, G. G., Ovcharenko, I., Pachter, L., Dubchak, I., and Rubin, E. M. (2002) *Genome Res.* **12,** 832–839
46. Suliman, H. B., Sweeney, T. E., Withers, C. M., and Piantadosi, C. A. (2010) *J. Cell Sci.* **123,** 2565–2575
47. Suliman, H. B., Carraway, M. S., Tatro, L. G., and Piantadosi, C. A. (2007) *J. Cell Sci.* **120,** 299–308
48. Piantadosi, C. A., Carraway, M. S., and Suliman, H. B. (2006) *Free Radic. Biol. Med.* **40,** 1332–1339
49. Wang, X., Tang, X., Gong, X., Albanis, E., Friedman, S. L., and Mao, Z. (2004) *Gastroenterology* **127,** 1174–1188
50. Czubryt, M. P., McAnally, J., Fishman, G. I., and Olson, E. N. (2003) *Proc. Natl. Acad. Sci. U.S.A.* **100,** 1711–1716
51. Lee, B. S., Heo, J., Kim, Y. M., Shim, S. M., Pae, H. O., Kim, Y. M., and Chung, H. T. (2006) *Biochem. Biophys. Res. Commun.* **343,** 965–972
52. Ricchetti, G. A., Williams, L. M., and Foxwell, B. M. (2004) *J. Leukoc. Biol.* **76,** 719–726
53. Lo, S. C., Li, X., Henzl, M. T., Beamer, L. J., and Hannink, M. (2006) *EMBO J.* **25,** 3605–3617
54. Ramachandran, B., Yu, G., and Gulick, T. (2008) *J. Biol. Chem.* **283,** 11935–11946
55. Carré, J. E., Orban, J. C., Re, L., Felsmann, K., Iffert, W., Bauer, M., Suliman, H. B., Piantadosi, C. A., Mayhew, T. M., Breen, P., Stotz, M., and Singer, M. (2010) *Am. J. Respir. Crit. Care Med.* **182,** 745–751
56. Reynolds, C. M., Suliman, H. B., Hollingsworth, J. W., Welty-Wolf, K. E., Carraway, M. S., and Piantadosi, C. A. (2009) *Free Radic. Biol. Med.* **46,** 564–572
57. Ranatunga, D., Hedrich, C. M., Wang, F., McVicar, D. W., Nowak, N., Joshi, T., Feigenbaum, L., Grant, L. R., Stäger, S., and Bream, J. H. (2009) *Proc. Natl. Acad. Sci. U.S.A.* **106,** 17123–17128
58. Gozzelino, R., Jeney, V., and Soares, M. P. (2010) *Annu. Rev. Pharmacol. Toxicol.* **50,** 323–354
59. Dhingra, S., Sharma, A. K., Arora, R. C., Slezak, J., and Singal, P. K. (2009) *Cardiovasc. Res.* **82,** 59–66
60. Deng, J., Kohda, Y., Chiao, H., Wang, Y., Hu, X., Hewitt, S. M., Miyaji, T., McLeroy, P., Nibhanupudy, B., Li, S., and Star, R. A. (2001) *Kidney Int.* **60,** 2118–2128
61. Brooks, D. G., Trifilo, M. J., Edelmann, K. H., Teyton, L., McGavern, D. B., and Oldstone, M. B. (2006) *Nat. Med.* **12,** 1301–1309
62. Brouard, S., Otterbein, L. E., Anrather, J., Tobiasch, E., Bach, F. H., Choi, A. M., and Soares, M. P. (2000) *J. Exp. Med.* **192,** 1015–1026
63. Piantadosi, C. A., and Suliman, H. B. (2006) *J. Biol. Chem.* **281,** 324–333
64. Scarpulla, R. C. (2008) *Physiol. Rev.* **88,** 611–638
65. Liochev, S. I., and Fridovich, I. (1997) *Free Radic. Biol. Med.* **23,** 668–671
66. Dasgupta, J., Subbaram, S., Connor, K. M., Rodriguez, A. M., Tirosh, O., Beckman, J. S., Jourd'Heuil, D., and Melendez, J. A. (2006) *Antioxid. Redox Signal* **8,** 1295–1305
67. Cauwels, A., Janssen, B., Waeytens, A., Cuvelier, C., and Brouckaert, P. (2003) *Nat. Immunol.* **4,** 387–393
68. Bradley, J. R. (2008) *J. Pathol.* **214,** 149–160
69. Zhang, L., Yu, J., Park, B. H., Kinzler, K. W., and Vogelstein, B. (2000) *Science* **290,** 989–992
70. Bruey, J. M., Bruey-Sedano, N., Luciano, F., Zhai, D., Balpai, R., Xu, C., Kress, C. L., Bailly-Maitre, B., Li, X., Osterman, A., Matsuzawa, S., Ter-

skikh, A. V., Faustin, B., and Reed, J. C. (2007) *Cell* **129,** 45–56
71. Sarady, J. K., Zuckerbraun, B. S., Bilban, M., Wagner, O., Usheva, A., Liu, F., Ifedigbo, E., Zamora, R., Choi, A. M., and Otterbein, L. E. (2004) *Faseb J.* **18,** 854–856
72. Stumpo, R., Kauer, M., Martin, S., and Kolb, H. (2003) *Cytokine* **24,** 46–56
73. Dinkova-Kostova, A. T., Holtzclaw, W. D., Cole, R. N., Itoh, K., Wakabayashi, N., Katoh, Y., Yamamoto, M., and Talalay, P. (2002) *Proc. Natl. Acad. Sci. U.S.A.* **99,** 11908–11913
74. Zhang, D. D., and Hannink, M. (2003) *Mol. Cell. Biol.* **23,** 8137–8151
75. Li, M. H., Jang, J. H., Na, H. K., Cha, Y. N., and Surh, Y. J. (2007) *J. Biol. Chem.* **282,** 28577–28586
76. Zhang, X., Shan, P., Alam, J., Fu, X. Y., and Lee, P. J. (2005) *J. Biol. Chem.* **280,** 8714–8721
77. Dinarello, C. A. (2010) *Eur. J. Immunol.* **40,** 599–606
78. Schroder, K., and Tschopp, J. (2010) *Cell* **140,** 821–832
79. Martinon, F., Burns, K., and Tschopp, J. (2002) *Mol. Cell* **10,** 417–426
80. Kanneganti, T. D., Lamkanfi, M., Kim, Y. G., Chen, G., Park, J. H., Franchi, L., Vandenabeele, P., and Núñez, G. (2007) *Immunity* **26,** 433–443
81. Pajkrt, D., Camoglio, L., Tiel-van Buul, M. C., de Bruin, K., Cutler, D. L., Affrime, M. B., Rikken, G., van der Poll, T., ten Cate, J. W., and van Deventer, S. J. (1997) *J. Immunol.* **158,** 3971–3977
82. Brandtzaeg, P., Osnes, L., Ovstebø, R., Joø, G. B., Westvik, A. B., and Kierulf, P. (1996) *J. Exp. Med.* **184,** 51–60
83. Lowe, P. R., Galley, H. F., Abdel-Fattah, A., and Webster, N. R. (2003) *Crit. Care Med.* **31,** 34–38
84. Shin, H. D., Winkler, C., Stephens, J. C., Bream, J., Young, H., Goedert, J. J., O'Brien, T. R., Vlahov, D., Buchbinder, S., Giorgi, J., Rinaldo, C., Donfield, S., Willoughby, A., O'Brien, S. J., and Smith, M. W. (2000) *Proc. Natl. Acad. Sci. U.S.A.* **97,** 14467–14472
85. Ziegler-Heitbrock, L., Lötzerich, M., Schaefer, A., Werner, T., Frankenberger, M., and Benkhart, E. (2003) *J. Immunol.* **171,** 285–290
86. Unterberger, C., Staples, K. J., Smallie, T., Williams, L., Foxwell, B., Schaefer, A., Kempkes, B., Hofer, T. P., Koeppel, M., Lohrum, M., Stunnenberg, H., Frankenberger, M., and Ziegler-Heitbrock, L. (2008) *Mol. Immunol.* **45,** 3230–3237
87. Oka, S., Ago, T., Kitazono, T., Zablocki, D., and Sadoshima, J. (2009) *J. Mol. Med.* **87,** 785–791
88. Platzer, C., Fritsch, E., Elsner, T., Lehmann, M. H., Volk, H. D., and Prösch, S. (1999) *Eur. J. Immunol.* **29,** 3098–3104
89. Alvarez, Y., Municio, C., Alonso, S., Sánchez Crespo, M., and Fernández, N. (2009) *J. Immunol.* **183,** 1471–1479